The Journal of Experimental Biology 213, 2629-2639

doi:10.1242/jeb.043547

Sparse but specific temporal coding by spikes in an insect sensory-motor ocellar pathway

Peter J. Simmons[1,*] and Rob R. de Ruyter van Steveninck[2]

[1]Institute of Neuroscience and School of Biology, Newcastle University, Newcastle upon Tyne, NE1 7RU, UK and
[2]Department of Physics, Indiana University, Bloomington IN 47405, USA

*Author for correspondence (p.j.simmons@ncl.ac.uk)

Accepted 21 April 2010

SUMMARY

We investigate coding in a locust brain neuron, DNI, which transforms graded synaptic input from ocellar L-neurons into axonal spikes that travel to excite particular thoracic flight neurons. Ocellar neurons are naturally stimulated by fluctuations in light collected from a wide field of view, for example when the visual horizon moves up and down. We used two types of stimuli: fluctuating light from a light-emitting diode (LED), and a visual horizon displayed on an electrostatic monitor. In response to randomly fluctuating light stimuli delivered from the LED, individual spikes in DNI occur sparsely but are timed to sub-millisecond precision, carrying substantial information: 4.5–7 bits per spike in our experiments. In response to these light stimuli, the graded potential signal in DNI carries considerably less information than in presynaptic L-neurons. DNI is excited in phase with either sinusoidal light from an LED or a visual horizon oscillating up and down at 20 Hz, and changes in mean light level or mean horizon level alter the timing of excitation for each cycle. DNI is a multimodal interneuron, but its ability to time spikes precisely in response to ocellar stimulation is not degraded by additional excitation. We suggest that DNI is part of an optical proprioceptor system, responding to the optical signal induced in the ocelli by nodding movements of the locust head during each wing-beat.

Key words: information, precision, spike, coding, flight, ocellus, locust.

INTRODUCTION

In neuronal pathways that connect sensory with motor systems, an important transformation is the conversion of graded potentials into spikes. This transformation can occur within the receptor cells themselves if they have long axons but often occurs in second- or third-order neurons such as ganglion cells in the vertebrate retina or medullary neurons in the insect optic lobe. Receptor potentials and other graded changes in membrane potential provide an analogue representation of signal strength, but the distances over which they can communicate are limited, and propagating spikes are needed to convey signals between different regions of a nervous system. By using a rate code (Adrian and Zotterman, 1926), spike trains can signal variations in signal strength, but individual spikes can also mark the occurrence of particular events such as stimulus features. We would expect that, where spikes are used in a rate code to report changes in stimulus strength, they would be quite frequent, but, where they are used to specify particular stimulus features, individual spikes would occur more sparsely, with their time precisely controlled. The times of spikes clearly matter when it is important to preserve temporal aspects of a signal, such as in auditory systems (Carr, 1993; Pollak et al., 1977; Carr and Konishi, 1990; Mason et al., 2001; Rokem et al., 2006) or electrosensory systems (Rose and Heiligenberg, 1985; Carr et al., 1986). But precision in spike timing has also been found in other sensory systems where the need for temporal fidelity is not so clear, including somatosensory systems (Petersen et al., 2001; Montemurro et al., 2007), mechanosensory systems (Billimoria et al., 2006), olfactory systems (Cassenaer and Laurent, 2007) and visual systems (Bair and Koch, 1996; Liu et al., 2001; Nemenman et al., 2008). We investigate here the nature of the spike code that is used in an identified neuron that converts sensory signals in the form of graded changes in potential into spikes for transmission to motor centres.

Estimates of information carrying capacity (e.g. Rieke et al., 1997; Borst and Theunissen, 1999) indicate that graded potential signals have a greater information carrying capacity than spike trains, but there have been few measurements at different stages within defined pathways, and most come from arthropods. In a spider mechanosensory neuron, spike trains carry considerably less information about the stimulus than the graded receptor potentials (Juusola and French, 1997). In the fly retina, second-order lamina monopolar cells carry information at rates as high as 1650 bits s^{-1} in graded potential signals (de Ruyter van Steveninck and Laughlin, 1996). There are no measurements from their immediate postsynaptic targets, but, in the lobula plate, the identified neuron, H1, carries 80 bits s^{-1} in spike trains (de Ruyter van Steveninck et al., 1997), and each spike carries 1.5 bits of information (Fairhall et al., 2001). Although H1 generates continual trains of spikes in response to moving visual panoramas, spike timing is consistent between repetitions of the same stimulus (e.g. de Ruyter van Steveninck et al., 1997; Warzecha et al., 1998), which is responsible for relatively high rates of information transmission (Nemenman et al., 2008). Also in the fly lobula plate are some motion-sensitive neurons that operate with graded changes in membrane potential, and others generate trains of spikes, and information carrying capacity is higher in the neurons that use graded potentials than in the neurons that use spike trains (Haag and Borst, 1997; Haag and Borst, 1998). In the turtle retina, graded potential changes also carry information at a greater rate than spike trains (Dhingra and Smith, 2004).

Axons in the insect nerve cord provide clearly identifiable links between sensory and motor systems. Those that have been investigated so far mainly signal with bursts of spikes, for example:

in cockroach giant interneurons, the relative number of spikes triggered within a few tens of milliseconds by a gust of wind is the key parameter in determining the direction in which a cockroach turns (Liebenthal et al., 1994; Levi and Camhi, 2000); the locust looming sensitive visual DCMD neuron generates a burst of spikes whose rate tracks the approach of an object towards the eye (e.g. Rind and Simmons, 1992; Judge and Rind, 1997; Peron and Gabbiani, 2009); and optomotor neurons in the nerve cord and optic lobes produce spikes whose rate depends on the speed of image movement [e.g. locust (Kien, 1974; Rind 1990); moth (Rind, 1983); fly (Haag et al., 2007; Wertz et al., 2008)]. The neuron that we study, DNI, has an axon in the nerve cord of the locust, and both the cell body in the brain and the axon in the nerve cord are accessible to electrophysiological experiments.

DNI (Fig. 1) is in the ocellar pathway, which offers particular advantages in studying neuronal coding because it is a simple pathway in which signals at each stage between photoreceptors to motor neurons can be recorded and related to behavioural responses. DNI belongs to a group of neurons called deviation (DN) detectors because they respond to movements of an artificial horizon (e.g. Griss and Rowell, 1986; Rowell and Reichert, 1986). Support for the idea that they correct deviation from flight course comes from the observations that they connect with wing motor neurons (Simmons, 1980), and stimulating their axons changes the relative timing of spikes in different wing motor neurons (Hensler and Rowell, 1990). DNI is excited when light directed at the median or ipsilateral ocellus is dimmed, which occurs when the locust pitches downward with respect to the visual horizon, and by wind directed over the head (Simmons, 1980; Rowell and Reichert, 1986). The optical design of the ocelli (single-lens eyes that adult locusts have as well as compound eyes) ensures that they collect light from a wide area, and their second-order 'L-neurons' are extremely sensitive to changes in light, suggesting that they report alterations in the angle of the visual horizon by responding to fluctuations in the amount of light each ocellus receives (Wilson, 1978a). Graded potentials are transferred across synapses between photoreceptors and L-neurons (Simmons, 1995), and then from L-neurons to DNI and two other DN neurons on each side (Simmons, 1981; Simmons, 1993). The graded potential carried by L-neurons provides a faithful record of fluctuations in light up to at least 50 Hz (Simmons, 1993), and then DNI converts the graded potential representation of the sensory stimulus into spikes that travel down the nerve cord. Responses by DN neurons to moving horizons have been previously recorded over time-scales that would last several wing-beats (e.g. Rowell and Reichert, 1986; Hensler, 1992). We found that DNI generates spikes relatively sparsely but timed with remarkable accuracy, and we suggest that the timing of individual spikes in DNI provides a reliable indication of changes in pitch on a wing-beat by wing-beat basis.

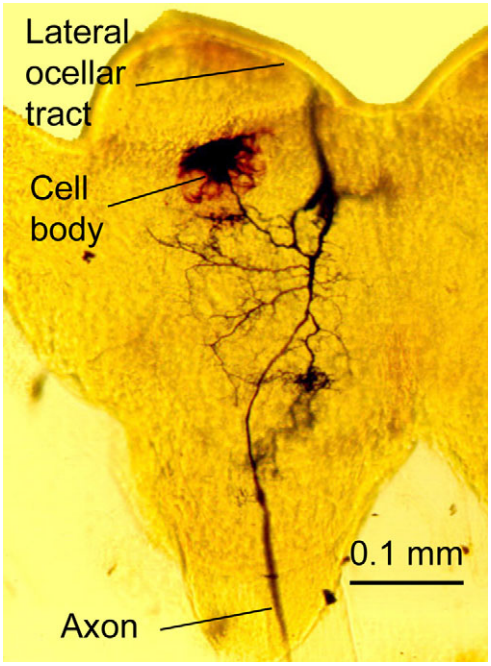

Fig. 1. Photograph of a DNI neuron in the brain. The neuron was stained by intracellular injection of cobalt and silver intensification (see Simmons, 1981). We focus in this paper on the way axonal spikes encode information. DNI receives graded potentials at synapses with ocellar L-neurons in the lateral ocellar tract and converts those potentials into spikes that travel to the thoracic ganglia.

MATERIALS AND METHODS

We analyzed results from 45 experiments on adult *Schistocerca gregaria* (Forskål) from a crowded colony at Newcastle University, UK. We made intracellular recordings from the cell body of DNI or from L-neurons in the brain, or from the axon of the DNI in the nerve cord, as described previously (Simmons, 1980; Simmons, 1993). We identified DNI by the location of its cell body or axon, and by its responses to illumination from either the ipsilateral or median ocellus and to puffs of air. The locusts were kept at a temperature of 24–26°C.

We delivered light stimuli using a bright-green light-emitting diode (peak wavelength 525 nm, maximum intensity 17,000 mcd; Yoldal) held 50 mm from the ocellus and directed at its lens. The light-emitting diode (LED) was calibrated using a Radiometer (Ealing). We controlled stimuli and acquired data using a Micro1401 with Spike2 for Windows Software (Cambridge Electronic Design). To analyze data, we used MatLab (the Mathworks Inc.) and SigmaPlot (SPSS), and we used MatLab routines to generate white noise stimuli. In most experiments, the frequency power spectral density of the light stimulus was cut off at 80 Hz, but spectral distributions that were flat to at least 500 Hz yielded results indistinguishable from those at 80 Hz. The intensity had a Gaussian distribution. Usually the stimulus was a sequence 2.048 s in length that was delivered repeatedly, enabling us to determine the mean responses and noise at different stages in the ocellar pathway.

To analyze the information conveyed by a single spike, we repeated the same Gaussian stimulus multiple times in order to get a reliable estimate of the time varying spike rate in discrete time bins. Here, we recorded spike occurrences in bins down to Δt=0.2 ms wide. *A priori* a single spike could fall with uniform probability in any of $T/\Delta t$ bins, which means that the *a priori* uncertainty, or total entropy, is $-\log_2(T/\Delta t)$ bits. From the timing of a single spike on $[0,T]$, distributed with a density proportional to the time varying rate, we get a corresponding noise entropy. The information in a single spike, I_{spike}, is the difference between these entropies, calculated as:

$$I_{\text{spike}} = \frac{1}{T}\int_0^T \frac{r(t)}{\bar{r}} \log_2\left[\frac{r(t)}{\bar{r}}\right] \mathrm{d}t \qquad (1)$$

(Brenner et al., 2000), where $r(t)$ is the time varying spike rate, and $\bar{r}$ is the time-averaged spike rate. To analyze the information rate transmitted by graded potentials, we used the same method we used previously (Simmons and de Ruyter van Steveninck, 2005), based

on Shannon's (Shannon and Weaver, 1949) result for Gaussian channels:

$$R = \int_0^\infty \log_2\left[1 + \frac{S(f)}{N(f)}\right] df \ , \qquad (2)$$

where R is the information transmitted (in bits s^{-1}), and f is frequency (Hz).

In some experiments, an ocellus was stimulated with a moving horizon displayed on an electrostatic monitor. The visual pattern was generated with a VSG2/1 and RG2 card (Cambridge Research Systems) in a PC, and displayed on a green COS1611 monitor (Kikusui), with a refresh rate of 200 Hz. The horizon was a straight border between a light and a darker area of the screen, and, in most experiments, we oscillated it up and down in a sinusoidal manner. The sub-tense of the screen at the ocellus was 65×55 deg, and the surface of the screen was 45 deg to the long axis of the locust. The intensities of 'sky' and 'ground' measured at the ocellus were 0.013 and 0.005 mW cm^{-2}.

Puffs of air were delivered with a pipe of 0.5 cm inner diameter positioned 5 cm from the head, using a compressed air supply controlled by a solenoid valve. The peak velocity of puffs at the head was 2 m s^{-1}, measured using a Skymate SM018 anemometer (Ambient Weather, AZ, USA).

RESULTS

Sparse but precisely timed spikes

To characterize the relationship between light stimuli and spikes produced by DNI, we recorded from its axon just anterior to the mesothoracic ganglion, delivering light stimuli to the ipsilateral ocellus from a LED. We found that DNI generates spikes relatively sparsely in response to light stimuli and that the timing of individual spikes is tightly regulated. This indicates that the signal DNI conveys to thoracic motor control networks marks particular features in the stimulus rather than recording light intensity.

The experiment from which the excerpts in Fig. 2A come illustrates the sparseness of DNI spikes. We delivered 27 s long random light stimuli and scaled the same waveform to produce stimuli of different mean intensities and contrasts. For a mean intensity of 35 μ W cm^{-2}, mean spike rate was 24.1 spikes s^{-1} at stimulus contrast (c) 0.24, and 13.0 spikes s^{-1} at c 0.12. A brighter stimulus, mean intensity 205 μW cm^{-2}, caused lower mean spike rates: 7 spikes s^{-1} at c 0.24, and 3 spikes s^{-1} at c 0.12, values that were typical of 10 experiments. The maximum spike rate we recorded was 25/s, and, under steady illumination, DNI spiked at less than 0.1/s. The DNI axon would not perform well in reporting light intensity, being limited in following slow changes by adaptation in L-neurons (Wilson, 1978b; Simmons, 1993) and in following fast changes by low spike frequency.

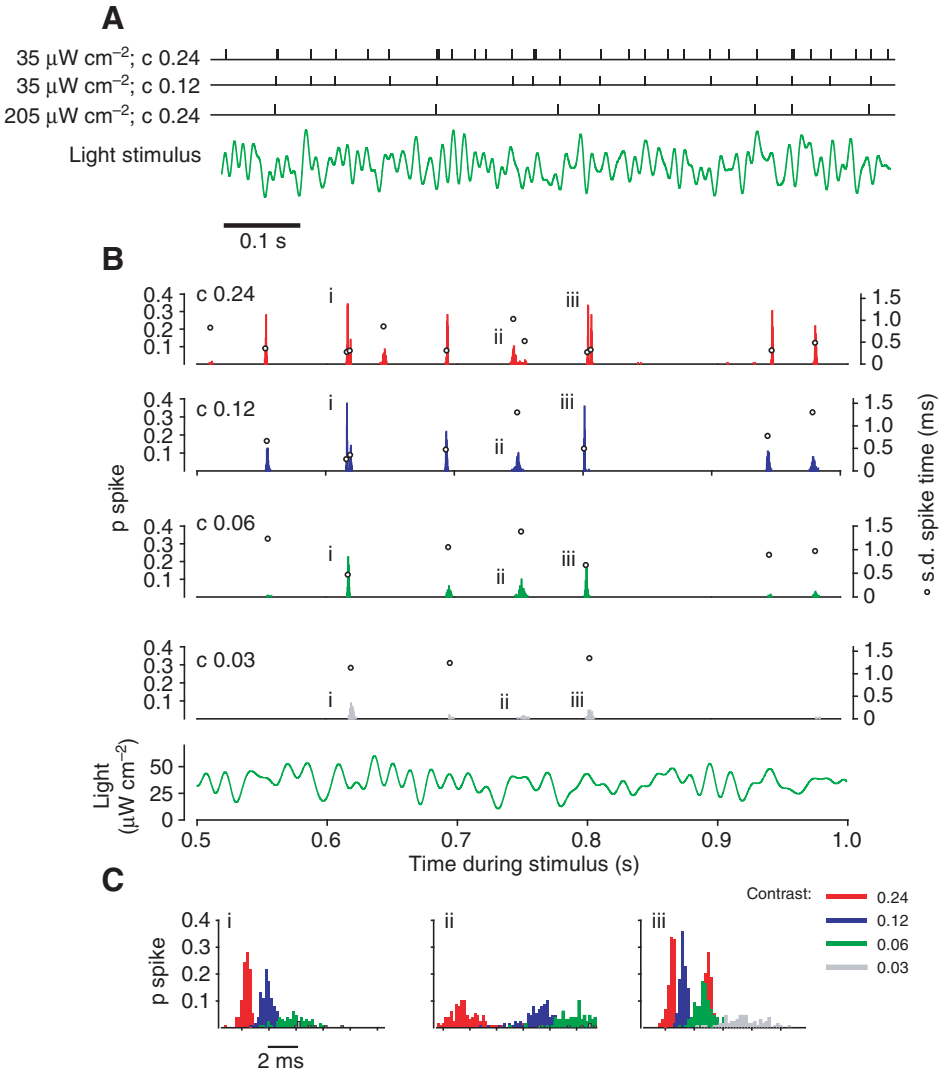

Fig. 2. DNI spikes are sparse and precisely timed. (A) Each row of small vertical lines indicates times of spikes in response to a fluctuating light stimulus; 1 s excerpts from stimuli of duration 27 s are shown. The stimulus waveform shown was scaled to different mean intensities and contrasts, indicated on the left. Note the relatively low numbers of spikes in each response. (B) Consistency of spike times in response to light stimuli. Spikes recorded from the pro-mesothoracic axon were collected in 0.2 ms bins. 1 s excerpts are shown from 128 repetitions of a 2.48 s duration Gaussian-modulated light stimulus (mean 35 μW cm^{-2}, high-frequency cut-off at 80 Hz) with four different contrasts ('c'). The standard deviation of spike time is plotted (open circles) for each histogram peak (or spike cluster). Light stimulus for mean intensity 35 μW cm^{-2}, c 0.24 is shown. (C) Spike clusters i–iii identified in B for each stimulus contrast (identified by colour) plotted on an expanded time-scale.

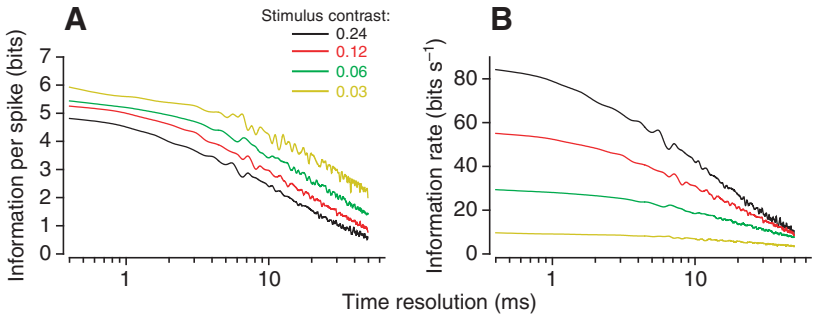

Fig. 3. Estimates of information per DNI spike (A) and rate of information carried by the DNI axon (B) plotted against temporal resolution. Plots were made from the experiment shown in Fig. 2B,C.

To investigate whether DNI is likely to use spike time as a signal, we showed that individual spikes are generated at remarkably consistent times when the same, randomly varying, stimulus was repeated (Fig. 2B,C). Each 2.048 s stimulus was repeated 128 times. Consistency in response is shown by the tight clustering of time bins in which spikes occurred through a sequence of identical stimuli, usually one spike per cluster on each repetition. Most bins contained no spikes – 94% of bins at c 0.24 and 98% at c 0.03 contained no spike. Three individual clusters are shown on an expanded time-scale in Fig. 2C. Lower contrast stimuli produced fewer spikes, and the latency and standard deviation of spike times (s.d.$_{sp}$) were greater than for higher contrast stimuli. In clusters shown in Fig. 2A, we measured average s.d.$_{sp}$ for different stimulus contrasts as 0.47 ms, c 0.24; 0.68 ms, c 0.12; 0.97 ms, c 0.06; and 1.45 ms, c 0.03, with similar measurements in five different locusts. In other locusts, spike time drifted during delivery of stimulus sequences, owing to adaptation to mean stimulus light levels, which can have a time-course of several hours (Wilson, 1978c).

In response to sinusoidal light stimuli between 10 and 30 Hz, DNI usually produced a single spike at a consistent time during each cycle. The distribution of spike times was similar to that for randomly fluctuating stimuli and increased as stimulus contrast decreased: from one experiment with stimulus frequency 20 Hz, s.d.$_{sp}$ was 0.42 ms at c 0.2; 0.45 ms at c 0.1; 0.55 ms at c 0.05; and 1.7 ms at c 0.025. Stimulus frequency also affected s.d.$_{sp}$: for stimuli c 0.1, s.d.$_{sp}$ was 0.40 ms at 30 Hz, rising to 0.45 ms at 20 Hz and to 0.95 ms at 10 Hz.

A second measure of spike precision is from an estimate of the information each carries (Fig. 3A), which we obtained by subtracting noise entropy from total entropy in spike times in responses to the repeated stimulus shown in Fig. 2B (Strong et al., 1998; Brenner et al., 2000). We estimate that each spike carries between 4.5 and 7 bits of information, being highest for higher-stimulus contrasts. At a sampling resolution of 1 ms (where the gradient of the curve of resolution against information flattens, Fig. 3A), information per spike was: 4.4 bits at c 0.24; 4.9 bits at c 0.12; 5.2 bits at c 0.06; and 5.6 bits at c 0.03. Similar estimates of information per spike were found in 12 different experiments, with the maximum information per spike varying between 4 and 7 bits. It is safe, therefore, to accept that, in responding to the stimuli that we delivered, each DNI spike carried approximately 5 bits of information. Higher contrast stimuli generate greater numbers of DNI spikes than lower contrast stimuli, and thus, at high stimulus contrasts, DNI spike trains carry information at a greater rate than at low contrasts (Fig. 3B). At 1 ms resolution, information rate carried by spikes was: 77.8 bits s^{-1} at c 0.24; 58.1 bits s^{-1} at c 0.12; 27.9 bits s^{-1} at c 0.06; and 9.1 bits s^{-1} at c 0.03.

Information in the underlying postsynaptic potential

Within DNI, the graded synaptic input signal from L-neurons is converted into axonal spikes. We have previously estimated that L-neurons and the excitatory output synapses they make carry information at several hundred bits per scond (Simmons and de Ruyter van Steveninck, 2005), or about four to five times greater than the information carrying capacity of trains of spikes in the DNI axon. To gain some further insight into information transmission within the ocellar pathway, we estimated the rate of information carried in underlying graded potential of the DNI, recorded from its cell body (individual postsynaptic processes are too small for stable recordings). We injected hyperpolarizing current to suppress spikes and reveal the underlying, sub-threshold responses to stimuli (Fig. 4A,B). In most experiments, a –5 to –7 nA steady current was sufficient to stop spikes. The DNI response waveform was consistent between stimulus repetitions, shown by the five individual traces in pale blue, Fig. 4A. It usually had the appearance of discrete potentials of variable amplitude, each one with a more rapid depolarizing phase than the hyperpolarizing phase, a shape that is reflected in the skew of the voltage level distribution (Fig. 4A). This type of response was recorded irrespective of the power spectrum of the light waveform, so was not an artefact of too low a stimulus frequency. Two factors that could contribute to this waveform characteristic are rectification in the input resistance of the DNI (Simmons, 1993) and sub-threshold regenerative responses. The skew in voltage level distribution was too great in two out of every three experiments for us to make reasonable estimates of information rates.

As in our previous experiments on graded potentials in L-neurons (Simmons and de Ruyter van Steveninck, 2005), we estimated information by dividing the power spectral density of the mean signal in DNI by the mean of the power spectral densities of noise (Shannon and Weaver, 1949; de Ruyter van Steveninck and Laughlin, 1996). From Fig. 4B, we estimate that the graded potential in DNI carries 85 bits s^{-1} in response to fluctuating light, and we made similar estimates in four different experiments (range 72–85 bits s^{-1}). This indicates that the information rate carried by graded potentials recorded from the cell body of the DNI is considerably less than the capacity of excitatory synaptic output connections made by L-neurons (Simmons and de Ruyter van Steveninck, 2005).

Characterizing light signals that trigger DNI spikes

Because DNI spikes are infrequent, each is likely to signify a particular feature of a light stimulus. To identify this feature, we generated spike-triggered averages for the light waveforms shown in Fig. 2A. In Fig. 5A, the light preceding spikes during one of these stimuli of length 27 s is shown, with the grey band indicating one standard deviation (s.d.) greater and smaller than the mean, and the black lines showing the light preceding six individual spikes. Here, c was 0.24 and mean intensity was 35 μW cm^{-2}. The average light waveform was biphasic, approximately a sinusoid with frequency approximately 30 Hz, but individual stimuli vary considerably in

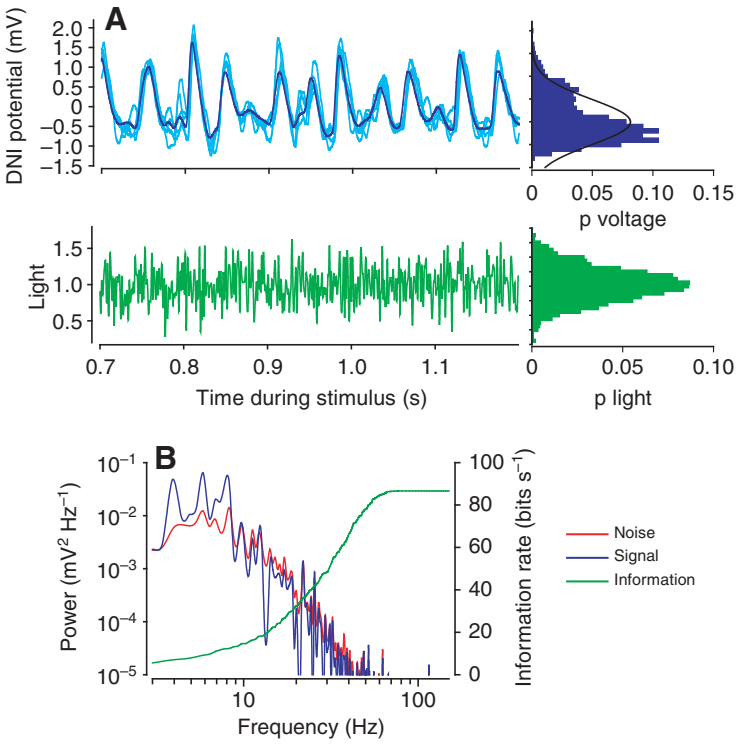

Fig. 4. Sub-threshold response by DNI to a Gaussian light stimulus and estimation of information in the response. (A) Average (blue) and five individual intracellular recordings (pale blue) from the cell body showing a 0.5 s excerpt of a 2.048 s stimulus. The stimulus was repeated 128 times; mean, 35 μW cm^{-2}, c 0.24 and flat power distribution to at least 500 Hz (axis for light is scaled with mean light at 1.0). To the right are plots of the probability distributions of voltage levels recorded from DNI (top) and of the light stimulus (bottom). (B) Estimate of information contained in the graded potential response. Signal-to-noise ratio was calculated by dividing the power spectral density of the mean signal in DNI by the average power spectral density of noise. This was used to calculate the cumulative information rate, as explained in the Materials and methods section.

shape. The most consistent stimulus feature is a rapid decrease in light intensity, crossing mean light intensity 25–32 ms before the spike. The s.d. of light intensity during this phase was about half that at other times in the spike-triggered waveform (0.27 light contrast units compared with 0.45–0.5). Inspection of individual light waveforms (green lines in Fig. 5A) shows that much of the variability here is due to the time of occurrence or the duration of a decrease in light rather than its rate of change. Spikes were triggered by decreases in light at a rate of between 0.08 and 1.4 contrast units per millisecond, so this is the stimulus feature most likely to trigger a DNI spike, particularly if the decrease in light occurs in the middle of a sinusoidal cycle of light change with a period of between 30 and 50 ms.

For different stimulus contrasts, the peaks of the average signature waveform alter in amplitude (Fig. 5B), with the effect that the responses span the contrast of the stimulus (Fig. 5C). The delay between the positive and negative peaks in light waveform does not alter, suggesting that the ocellar pathway adapts to different speeds of decrease in light when the mean contrast in a signal changes. When we compared responses at two different mean light intensities, we found that the delay between light waveform and a spike decreased a small amount, approximately 1 ms for 35 μW cm^{-2} compared with 508 μW cm^{-2} (Fig. 5B, unbroken green and dark-green lines).

We also compared frequency responses to sinusoidal stimuli by axonal spikes in DNI and by presynaptic L-neurons (Fig. 5D,E). Stimuli at frequencies below 4 Hz generated no spikes, whereas stimuli at 10 Hz reliably triggered one spike per cycle. As stimulus frequency increased to 30 Hz, each cycle produced one spike, with a small number triggering two spikes 5 ms or less apart. For stimulus frequencies greater than 30 Hz, the probability of a spike on each cycle declined steeply. By comparison, the graded potential response by L-neurons is more broadly tuned (Fig. 5D,E). L-neurons respond well to stimuli with frequencies of 2 Hz or less, and the fall-off in response at high stimulus frequencies is less steep than that for DNI spikes (Fig. 5E).

Responses to movements of a visual horizon

Our results show that spikes in DNI mark the times at which light decreases significantly, and that DNI does this well over a range of frequencies of 10–30 Hz (Fig. 5E). Because the wing-beat frequency of a locust is approximately 20 per second (Weis-Fogh, 1956), it occurred to us that DNI might respond well to light modulation caused on each wing-beat. Light received by the median and lateral ocelli from the frontal part of the visual field might change rhythmically if during flight each wingbeat causes the head to nod or rock in the pitch plane. To investigate this idea, we first recorded responses from ocellar neurons to a moving horizon and then recorded responses to light from the LED in which sinusoidal fluctuations at 20 Hz were superimposed on step changes in mean intensity. This would mimic the changes in ocellar illumination caused by rhythmic head nodding, superimposed on changes in the angle of pitch of the locust relative to a horizon during flight.

To create a moving horizon, we used an electrostatic monitor, with the top part of the screen illuminated and the bottom part dark. We moved the horizon so that its elevation changed in a sinusoidal way, and we made intracellular recordings separately from L-neurons and from the cell body of the DNI (Fig. 6A). As expected, an upward movement of the horizon (decreasing the light on the ocellus) depolarized L-neurons and DNI. The amplitude of the change in L-neuron potential altered with the angle of horizon movement, and all cycles triggered depolarizing potentials, and often spikes, in DNI. We found that an inverted or else a vertically oriented, sideways-moving horizon was as effective at eliciting responses from DNI and from L-neurons as a normal configuration,

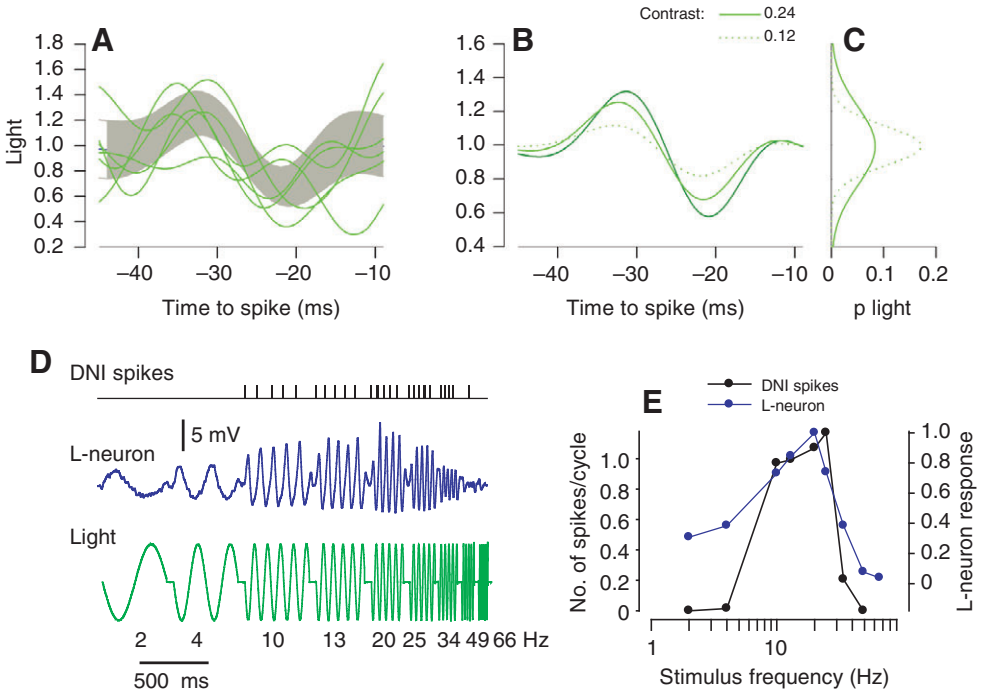

Fig. 5. Light stimuli that DNI spikes are tuned to. (A) Waveforms that precede DNI spikes produced in response to a Gaussian-modulated, non-repeating light stimulus. The grey band is average ± s.d. light waveform triggered from 650 spikes over 27 s, and each of the five green lines is the light waveform preceding an individual spike. Mean light intensity, 35 μW cm^{-2}, c 0.24. (B) Average waveforms for three different stimuli: green lines, mean intensity 35 μW cm^{-2} and c 0.24 (solid line; 650 spikes); c 0.12 (dotted line; 359 spikes); dark-green line, mean intensity 507 μW cm^{-2} and c 0.24 (191 spikes). Light units in A and B are relative to a mean of 1 for each stimulus intensity. Records from the same experiment as Fig. 2A. (C) Distributions of light during stimuli at c 0.24 and 0.12, corresponding with the green and dotted waveforms in B. (D) Responses to sinusoidal light at different frequencies (bottom) showing, from different experiments, spike times in a DNI axon (top) and intracellular responses by an L-neuron (second trace). (E) Plots from experiments illustrated in D of light frequency against number of DNI spikes per stimulus and L-neuron response amplitudes. The number of spikes was averaged from 110 cycles at each frequency; L-neuron response amplitudes were averaged from 15 cycles. Light mean intensity 35 μW cm^{-2} and c 0.2.

consistent with the observation that an L-neuron responds to light collected over a wide area rather than to optical features of an image (Wilson, 1978a).

The effects of the extent and frequency of horizon movement on spike production by a DNI axon are shown in Fig. 6B, which shows average responses from 50 movement cycles. The frequency tuning was similar to the tuning to sinusoidally changing light (Fig. 5E). Tested with a horizon moving 45 deg in elevation at frequencies between 15 and 30 Hz, most cycles of horizon movement caused a DNI spike, and, at higher frequencies, the response dropped sharply. Mean latency to a spike was 31.3 ms (s.d.$_{sp}$ 1.7 ms), measured from the point at which the horizon moved upwards through 0 deg elevation. Because there is jitter in the timing of stimulus movement on the screen, these measurements are less reliable than those for sinusoidal light from an LED. Fig. 7B also shows the effect of the change in elevation of the horizon during each movement, measured at a frequency of 20 Hz. For angles greater than 20 deg, the proportion of cycles that triggered spikes gradually rose, until, for movements of 37 deg or more, almost all cycles triggered a spike. These observations suggest that nodding movements of the head at flight frequency excite DNI, and the probability of a cycle of horizon movement triggering a spike depends on the extent of horizon movement.

We investigated whether the timing of spikes in DNI could provide a signal indicating a change in the attitude of a locust relative to the visual horizon. We stimulated ocelli with a moving horizon in five experiments and with sinusoidal light from an LED in these plus five others. Fig. 6C shows a recording from a DNI cell body while a horizon, oscillating by 5 deg at 20 Hz, stepped upwards and then downwards by 5 deg. This mimics nodding movements during flight, with changes in flight attitude superimposed. With the mean level of the horizon just below the centre of the screen, each cycle triggered a depolarizing response in DNI, but relatively few cycles triggered spikes. When the horizon jumped upwards in elevation by 5° (a decrease in mean ocellar illumination), the likelihood of a spike on each cycle increased. After 3 s, the horizon jumped downwards again, and the likelihood of spikes decreased. The delay between each cycle of movement and excitation also decreased as the mean horizon level shifted upwards.

To investigate in more detail the effect on DNI spike timing when an oscillating horizon shifts its mean elevation, we mimicked the effects of horizon movement with 20 Hz sinusoidal light from an LED (Fig. 6D,E). During a stimulus, the mean light was stepped between two levels every 0.5 s, and results were collected for 60 repetitions of the stimulus of duration 1 s. Spike delay was measured, as before, from the time at which light decreased past its mean intensity. Fig. 6D shows a sequence in which the light level stepped down for 0.5 s, equivalent to an upwards movement of a horizon over an ocellus, and then returned to the original level for 0.5 s. In this recording, the light stepped by 1.5 times the amplitude of the sinusoidal oscillation (mean light before step 35 μW cm^{-2} and contrast of sinusoidal light 0.2). Following a step downwards in light, most light cycles elicited a spike (dark dots), and the spike latency decreased, from a mean of 32.1 ms immediately before the

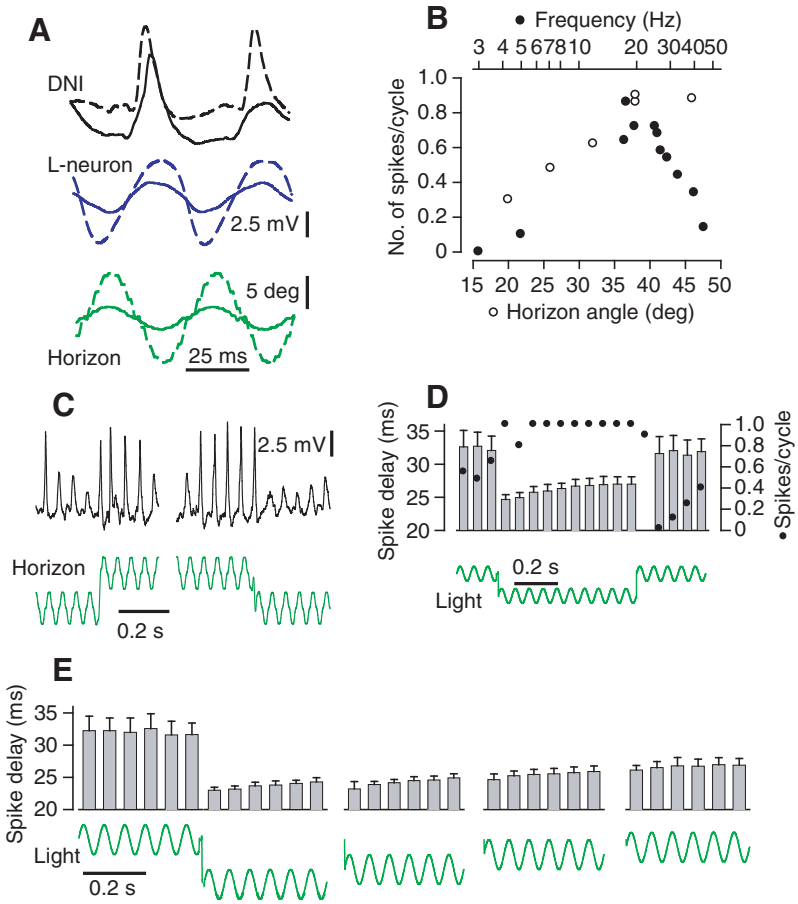

Fig. 6. Responses to horizon movements. (A) Intracellular responses recorded from a DNI cell body and from an L-neuron axon to 20 Hz oscillations of two amplitudes of a horizon displayed on an electrostatic monitor. (B) Plots of numbers of DNI axon spikes per stimulus cycle in response to the horizon oscillating at different frequencies (filled circles) or moving through different amplitudes (open circles). (C) Intracellular recording from a DNI cell body in response to a horizon oscillating at 20 Hz and stepping between two mean levels. There is a break of 2.2 s in the recording. (D) DNI axonal spikes in response to sinusoidally modulated light that jumped between different mean intensities, as shown by the records of light traces below the histograms. Jumps in mean intensity, 1.5 times the amplitude of the oscillations, occurred every 0.5 s. Histograms plot the mean delay to spikes for each cycle, and error bars indicate the standard deviation; dots indicate the mean number of spikes per stimulus cycle; 60 repetitions. (E) As D, but for four different downward-step amplitudes in light.

step to a mean of 24.7 ms for the cycle following the step. The mean latency increased slightly during the lower light level, to a mean of 28.3 ms just before the light level stepped upwards. Following the upward step, the first two light cycles usually triggered no DNI spikes, and then the number of cycles triggering a spike gradually increased, reaching 65% after 0.5 s, just before a downward step. Spike latency was fairly steady for those cycles that triggered spikes during the higher light level.

The change in latency following a step in light level depends on the amplitude of the step (Fig. 6E). Four different sizes of step from the same initial mean light level are shown (averages of 60 repetitions). For the sine wave cycle just before a downward step, mean spike latency was 31.6 ms (240 repetitions). For different step sizes relative to the sine wave amplitude, latencies for the first cycle following the step were: step 1.5, 24.7 ms; step 1.0, 25.0 ms; step 0.5, 27.3 ms; and step 0.25, 29.6 ms. This shows that changes in spike time elicited by rhythmical movements of the head can provide a signal about the extent of a change in flight attitude.

Robustness in spike timing

In addition to receiving inputs from ocellar L-neurons, the DNI is excited by wind-sensitive hairs on the head (Simmons, 1980; Rowell and Reichert, 1986). It is possible that its coding of light stimuli by precise timing of its spikes would be masked when DNI is excited through other stimulus modalities. We found, however, that the specificity of spike timing in DNI response to fluctuating light stimuli was preserved when the neuron was excited either by directing puffs of air at the head (Fig. 7A,B) or by depolarizing the current injected into its cell body (Fig. 7C,D).

The wind stimulus we used elicited 15–20 spikes s^{-1} at the start of each puff, delivered during steady illumination. Because the response adapted strongly, we could not use randomly fluctuating stimuli to investigate whether a wind stimulus affects the timing of spikes in response to a light stimulus. Instead, we compared responses to 200 cycles of sinusoidally modulated light without wind with responses to 200 cycles delivered during puffs of wind of duration 1 s (light stimulus 20 Hz, c 0.2, mean 35 $\mu W\,cm^{-2}$). Spike rasters of 20 stimulus cycles with and 20 without a wind stimulus are shown in Fig. 7A, and histograms showing the time of occurrence of the first spike during light stimuli with and without wind are shown in Fig. 7B. Without wind, each light cycle elicited a single spike. With the wind stimulus, 46% of the light cycles elicited two spikes separated by 3–5 ms, and the reminder elicited a single spike. The mean spike delay (measured as indicated in Fig. 7A) without wind was 22.5 ms, s.d.$_{sp}$ 1.0 ms, and with wind it was 21.4 ms, s.d.$_{sp}$ 3.16 ms for the first spike. Thus the wind stimulus shortened the mean spike delay slightly. The increase in variability in response to the light stimuli during wind is probably due to variability in the strength of, and response to, the wind rather than an effect directly on the DNI response to light stimuli.

To investigate in a more controlled manner whether excitation of DNI affects the way it responds to light stimuli, we depolarized a DNI by a steady injection of +5 nA into its cell body and compared the distribution of spikes with their distribution when no current was injected (Fig. 7C,D). We wished to discover whether the precision of spike time in response to ocellar stimuli would be masked in the presence of a relatively high background frequency of spikes in DNI. In accessing the DNI cell body, some

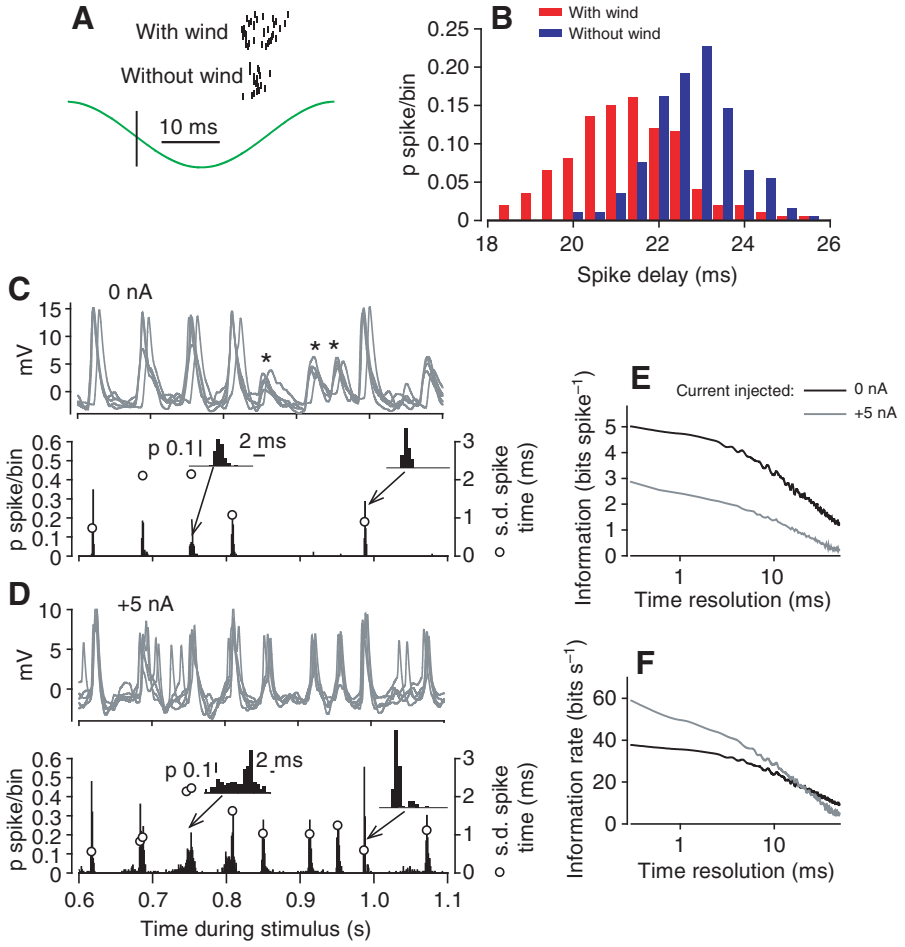

Fig. 7. Robustness of spike timing precision in response to light stimuli when DNI is excited by wind hair stimulation or current injection. (A,B) Comparison of DNI axonal spike responses to sinusoidal light stimuli (20 Hz; mean 35 μW cm^{-2}; c 0.1,) with and without an additional wind stimulus; A shows rasters of spikes in 20 light cycles, and B shows histograms of times of spikes from 200 light cycles in each condition. Time of spikes was measured relative to when light intensity decreased from its mean level during each cycle, as indicated by the vertical line in A. (C,D) Intracellular recordings from the DNI cell body with 0 nA (C) or +5 nA (D) current injected. In each, five traces of 0.5 s of responses to the stimulus are superimposed (grey). Asterisks indicate three discrete depolarizing potentials in C that each correspond with a spike in D. Below are corresponding spike probability histograms and their standard deviations; 98 stimulus repetitions in A, and 119 repetitions in B. The details of two corresponding spike time clusters are shown. Mean light was 35 μW cm^{-2}. (E,F) Estimate of information per spike (E) and information rate (F) in DNI responses to the light stimulus to show the effects of depolarising current.

of the nerves that carry wind-hair axons are cut, altering the responsiveness of the DNI. With positive current, the amplitude of spikes recorded from the cell body decreased, indicating that depolarization decreases input resistance, as described previously for ocellar L-neurons (Wilson, 1978b; Ammermüller and Zettler, 1986). The injected positive current increased mean spike frequency during light stimulation from 7.7 to 23.5 Hz. The same clusters of spikes apparent in responses to repeated sequences of fluctuating light when no current was injected (Fig. 7C) were all apparent when positive current was injected (Fig. 7D), and several new clusters appeared that corresponded with sub-threshold excitation of DNI in the absence of injected current (asterisks in Fig. 7C). Through 119 repetitions of the 2.048 s stimulus, we identified 17 clusters of spikes, and the positive current recruited spikes into an additional 16 clusters. In the original 17 clusters, s.d.$_{sp}$ was decreased by the current from 1.18 to 0.75 ms, and, in the 16 additional clusters, s.d.$_{sp}$ was 1.14 ms. With the depolarizing current, only approximately 10% of spikes occurred outside these clusters. Positive current decreased the information content per spike by about a half, from 4.7 bits to 2.4 bits (Fig. 7E), but increased the information rate carried by spike trains from 35 to 49 bits s^{-1}, measured at 1 ms resolution (Fig. 7F). The effects of injecting depolarizing current were reversible. We found similar effects in five different experiments. In some experiments, DC currents greater than 5 nA elicited spike rates up to 15/s under steady illumination, but these recordings were insufficiently stable to allow us to characterize responses to fluctuating light stimuli.

DISCUSSION

Our results show that each spike in DNI is a significant event: spikes are relatively rare, usually occur singly and are timed with considerable precision. DNI does not use trains of spikes to report a measure of light intensity, and it would not be possible to reconstruct a unique light stimulus from a train of DNI spikes. Instead, each spike marks a rapid, but not necessarily a sustained, decrease in the intensity of light reaching the ocelli. Because the timing is affected by stimulus frequency and contrast, it is likely that spike time relative to another event is the major code used by DNI to communicate to motor centres.

By clearly using a code in which spike timing rather than rate is significant, DNI differs from other interneurons in the insect nerve cord, where trains of spikes mediate behavioural responses [e.g. wind-sensitive cockroach giant interneurons (Liebenthal et al., 1994); bat-detecting cricket auditory neuron (Nolen and Hoy, 1984); collision-warning locust DCMD neuron (Santer et al., 2006)] and so shows that individual spikes in nerve cord axons can play significant roles in the sensory control of motor activity.

Performance and mechanism

DNI spike timing is precise, with a standard deviation often less than 1 ms, and this precision is reflected in an estimate of 4.5–7 bits

of information per spike, which is one of the highest values reported (Borst and Theunissen, 1999; van Rullen et al., 2005). The most accurate timings reported from nervous systems so far include the auditory system of parasitoid flies, which can resolve a time difference of 50 ns between signals in the two ears (Mason et al., 2001), and the behaviour and responses of various sensory neurons in bats, owls and electric fish (for a review, see Carr, 1993). Temporal resolution is important in these animals to enable spatial location of a source of sound or of electrical waves. Spikes in insect auditory receptors (Rokem et al., 2006) or axons in vertebrate auditory nerves are phase-locked to the stimulus waveform sound. Resolution is sometimes improved in higher-order neurons by signal averaging as a result of the convergence of many excitatory inputs onto a postsynaptic neuron (Carr and Konishi, 1990), although spike timing precision is not always preserved beyond primary auditory neurons. For example, in locusts, inter-trial variability of spike times in auditory receptors is as little as 0.15 ms at 30°C (Rokem et al., 2006), but responses by the local interneurons in the thoracic ganglia and by ascending brain neurons that these receptors drive are much more variable (Vogel et al., 2005). Similarly, in the owl auditory system, cochlea afferents carry spikes that are phase-locked to stimuli, but the precision of timing decreases considerably in the bursts of spikes produced in coincidence-detecting neurons in the nucleus laminaris and is restored in later stages by convergence (Christianson and Peña, 2006; Fischer and Konishi, 2008).

There are examples of precision in visual systems as well: in the fly H1 motion-sensitive neuron, spike timing can be precise at the millisecond level between stimulus repetitions (e.g. de Ruyter van Steveninck et al., 1997; Warzecha et al., 1998). In experiments in which the fly is rotated outdoors so it experiences natural light levels, it was shown that sub-millisecond precision of spike timing carries information about the motion stimulus (Nemenman et al., 2008). Under these conditions, the timing precision of H1 depends on the external optical signal-to-noise ratio (Lewen et al., 2001). Study of fast turning movements by flies suggests that their brains integrate optomotor stimuli over 30–50 ms (Collett and Land, 1985), so any significance of sub-millisecond spike precision by H1 for signal processing by its postsynaptic target neurons is not yet known. In the vertebrate visual system, retinal ganglion cells can carry over 4 bits per spike (Nirenberg et al., 2001), and mammalian lateral geniculate neurons carry up to 3.5 bits per spike (Reinagel and Reid, 2000; Liu et al., 2001), although these measurements have been made with rather unnatural visual stimuli in which the intensity of large patches of the visual field was changed.

A number of factors can influence the precision of spike timing and should be borne in mind in making comparisons. For DNI, we show here that light contrast and frequency both have significant effects, and temperature is also likely to have an effect (Simmons, 1990). Neuro-hormones affect spike precision in crustacean mechanoreceptors (Billimoria et al., 2006) and influence the responses of neurons involved in locust flight (e.g. Ramirez and Pearson, 1991; Rind et al., 2008), introducing the possibility that neuro-hormones released during natural flight will also affect responses by ocellar neurons.

We estimate that spikes in the DNI axon carry approximately 80 bits s^{-1} when spiking at a frequency of around 20 per second. A presynaptic L-neuron can carry approximately 300 bits s^{-1} (Simmons and de Ruyter van Steveninck, 2005), which indicates a loss of 60–80% in information between a graded potential in an L-neuron and spikes in a DN neuron axon. A large part of this loss is attributable to the way the synapse is used in transmitting information about fluctuations in light. The same type of excitatory synapse, made by L1-3 with L4-5 rather than with DNI, is capable of carrying information at up to 450 bits s^{-1}, but this capacity is achieved when the synapse is artificially depolarized from the threshold for transmitter release and operating in the linear part of its transfer curve. Moderate illumination hyperpolarizes L-neurons from the threshold for transmitter release (Simmons, 1993), so much of the signal is not usually transferred across the synapse to DNI as graded changes in potential. We estimate that the graded potential recorded from the DNI cell body carried 80 bits s^{-1} in response to fluctuating light in our experiments, indicating that the information in the graded potential signal is reduced by approximately two-thirds compared with that of an L-neuron. The reduction is probably not quite so severe for a number of reasons. First, the signal recorded from the cell body is conducted decrementally from the narrow postsynaptic branches in the ocellar tracts and has a lower bandwidth than that at the postsynaptic sites. Second, the signal-to-noise ratio might be inferior in the cell body compared with the postsynaptic sites owing to synaptic inputs from other dendritic regions of the neuron, such as those that receive inputs from wind-sensitive hairs. Third, we restricted measurements to a narrow range of potential changes in order to achieve a more normal distribution. Finally, even when the neuron is hyperpolarized, there are signs of small regenerative responses that alter the way the neuron responds to the neurotransmitter released by presynaptic L-neurons.

In transmission between an L-neuron and DNI, the nature of the signal in the ocellar pathway is altered from graded changes in potential that provide a measure of a fluctuating light stimulus into axonal spikes that mark the occurrence of significant decreases in light. Although under moderate illumination hyperpolarizing changes in potential are not transmitted across the synapse from L-neurons to DNI, these hyperpolarizing potentials are important in triggering rebound responses to decreases in light. When light decreases, L-neurons often generate small rebound spikes (Wilson, 1978b; Ammermüller and Zettler, 1986) whose amplitude depends on the size and duration of the hyperpolarization before the rebound (Simmons, 1982), and DN neurons also generate rebound spikes (Simmons, 1993). Together, the excitability of L-neurons and DNI ensures that the responses to sudden light decreases are enhanced and is probably the main factor that tunes the DNI frequency response to light stimuli at 10–30 Hz. At these frequencies, the gain of the tonically transmitting synapse is below maximum, which occurs for frequencies up to 10 Hz (Simmons and de Ruyter van Steveninck, 2005). The key to spike time precision in DNI, therefore, lies with the process that triggers rebound spikes in L-neurons. One feature that will help ensure that the excitatory drive to DNI from different L-neurons is synchronized is the inhibitory synapses that some L-neurons make with each other (Simmons, 1982; Simmons, 1986; Simmons, 2002).

The role of DNI in flight control

What is the significance of the DNI coding strategy of capping its spike rate at approximately 30 Hz and timing its spikes precisely? The wingbeat frequency of a locust is approximately 20 Hz (Weis-Fogh, 1956), so that DNI could be excited by regular movements of the head relative to the horizon during each wingbeat cycle. A small nodding movement of the head that modulates the amount of light reaching the ocelli from in front of the animal could cause this excitation. The light signal that L-neurons would receive in response to wing-beat-related head movements will depend on the amplitude and phase of head movements, on the effective contrast between sky and ground, and on the acceptance angle of L-neurons. Although it is likely that the head of a locust will nod in time with individual

wing-beats, we have no detailed recordings of locusts performing steady, unrestrained flight. A modelling study, which uses force measurements from tethered locusts, indicates that the angle of pitch of a free-flying locust will oscillate at wingbeat frequency (Taylor and Zbikowski, 2005). A number of high-definition recordings of locust swarms have been made for TV wildlife programs, but these show flight that is unsteady with frequent turns just after take-off. We have shown that DNI generates well-timed, sparse spikes in response to light signals from a green LED with contrasts of 0.1 or less, which is likely to be smaller than the contrast between sky and land. We showed that oscillations in the position of a horizon displayed on an electrostatic monitor by 5 deg or less are effective in triggering well-timed spikes in DNI, so it is reasonable to propose that DNI could receive a strong, exciting optical signal on each wing-beat. An alternative explanation is not obvious for the ability of DNI to generate single well-timed spikes in response to light signals oscillating near to the wing-beat frequency.

Step decreases in light to the median ocellus mediate large EPSPs in motor neurons of two particular depressor muscles for each wing: the dorsal longitudinal and the subalar, which also increases the angle of attack of the wing (Simmons, 1980), and these muscles could be used to counteract a pitch towards the ground. If the head nodding movements are combined with a change in the flight attitude of the locust, that will alter the timing of excitation to DNI, and so the timing of the excitation it delivers to those wing motor neurons. An advance in the timing or increase in the extent of their activation during a wing-beat to correct a change in flight attitude makes functional sense. Our results show that DNI can indicate deviation from level course by the timing of its spikes during each wing-beat; it would not use a rate code. Its ability to respond to signals greater than the wing-beat frequency will enable it to register within a single wing-beat that flight attitude has changed.

There is a precedent for a locust brain neuron able to respond during individual wing-beats. The tritocerebral giant interneuron is excited by frontal air currents and generates one or two spikes each wing-beat cycle as a result of a boost in air velocity caused by movements of the wings and possibly also by head nodding movements (Bacon and Möhl, 1979; Bacon and Möhl, 1983). It spikes during wing elevation in tethered, flying locusts. If DNI is excited in a similar way by wing-beat-related changes in air currents, and if the head also nods forwards during wing elevation, then two different modalities that excite DNI will coincide in time. Excitation of DNI during wing elevation would be appropriate for it to deliver excitation to wing depressor motor neurons during a wing-beat cycle. We showed that additional excitation to DNI, either by positive current injected into the cell body or from wind, does not mask the precision of spike timing in response to light stimuli. We believe that a phasic, proprioceptive role for a light-sensitive neuron, such as we propose for DNI, is novel. In other insects, ocellar neurons in the nerve cord are not so well known, but it is interesting that the median ocellus of dragonflies seems to have specializations that enhance vertical movements of the visual horizon (Berry et al., 2007). Relative timing of different modalities could be a mechanism by which a neuron uses measurement of physical qualities, such as light or wind, to make inferences about significant parameters, such as the angle of pitch.

A question of general significance in the sensory control of rhythmical movements such as flight concerns how information is delivered at an appropriate phase during the movement cycle. For example, in controlling the angle of pitch of a locust, it would be inappropriate to add excitation to wing depressor neurons during wing elevation, and the power output of a muscle during a wing-beat is sensitive to the phase of the wing-beat in which the muscle is excited by its motor neuron (Misizin and Josephson, 1987). Previously, it has been proposed that ocellar inputs to the flight system are gated through local thoracic interneurons, and that direct synapses between ocellar brain neurons such as DNI and motor neurons are of minor significance (Rowell and Pearson, 1983). However, DNI does cause large EPSPs in particular wing depressor motor neurons (Simmons, 1980). Our proposal that DNI is excited phasically on each wing-beat cycle by optically registering head nodding movements provides an alternative mechanism for gating the sensory stimulus. DNI clearly uses a code in which spikes are sparse but precisely timed. There is a limited time-window in each wing-beat cycle during which spikes can occur and can be effective at controlling motor outputs. This window is 5–10 ms in duration, which means that DNI, using a precision of 1 ms, is capable of generating 5–10 distinct signals during each wing-beat.

REFERENCES

Adrian, E. D. and Zotterman, Y. (1926). The impulses produced by sensory nerve endings: Part II: the response of a single end organ. *J. Physiol.* **61**, 151-171.

Ammermüller, J. and Zettler, F. (1986). Time-dependent and voltage-dependent currents in locust ocellar L-neurons. *J. Comp. Physiol. A* **159**, 363-376.

Bacon, J. and Möhl, B. (1979). Activity of an identified wind interneurone in a flying locust. *Nature* **278**, 638-640.

Bacon, J. and Möhl, B. (1983). The tritocerebral commissure giant (TCG) wind-sensitive interneurone in the locust-I. Its activity in straight flight. *J. Comp. Physiol. A* **150**, 439-452.

Bair, W. and Koch, C. T. (1996). Temporal precision of spike trains in extrastriate cortex of the behaving macaque monkey. *Neural Comput.* **8**, 1185-1202.

Berry, R., Stange, G., Oldberg, R. and van Kleef, J. (2006). The mapping of visual space by identified large second-order neurons in the dragonfly median ocellus *J. Comp. Physiol. A.* **192,** 1105-1123.

Billimoria, C. P., DiCaprio, R. A., Birmingham, J. T., Abbott, L. F. and Marder, E. (2006). Neuromodulation of spike-timing precision in sensory neurons. *J. Neurosci.* **26**, 5910-5919.

Borst, A. and Theunissen, F. E. (1999). Information theory and neural coding. *Nat. Neurosci.* **2**, 947-957.

Brenner, N., Bialek, W. and de Ruyter van Steveninck, R. R. (2000). Adaptive rescaling maximizes information transmission. *Neuron* **26**, 695-702.

Carr, C. E. (1993). Processing of temporal information in the brain. *Annu. Rev. Neurosci.* **16**, 223-243.

Carr, C. E. and Konishi, M. (1990). A circuit for detection of interaural time differences in the brainstem of the barn owl. *J. Neurosci.* **10**, 3227-3246.

Carr, C. E., Rose, G. and Heiligenberg, W. (1986). A time-comparison circuit in the electric fish midbrain. I. Behavior and physiology. *J. Neurosci.* **6**, 107-119.

Cassenaer, S. and Laurent, G. (2007). Hebbian STDP in mushroom bodies facilitates the synchronous flow of olfactory information in locusts. *Nature* **448**, 709-713.

Christianson, G. B. and Peña, J. L. (2006). Noise reduction of coincidence detector output by the inferior colliculus of the barn owl. *J. Neurosci.* **26**, 5948-5954.

Collett, T. S. and Land, M. F. (1985). Visual control of flight behaviour in the hoverfly *Syritta pipiens.* L. *J. Comp. Physiol.* **99**, 1-66.

de Ruyter van Steveninck, R. R. and Laughlin, S. B. (1996). The rate of information transfer at graded-potential synapses. *Nature* **379**, 642-645.

de Ruyter van Steveninck, R. R., Lewen, G. D., Strong, S. P., Koberle, R. and Bialek, W. (1997). Reproducibility and variability in neural spike trains. *Science* **275**, 1805-1808.

Dhingra, N. K. and Smith, R. G. (2004). Spike generator limits efficiency of information transfer in a retinal ganglion cell. *J. Neurosci.* **24**, 2914-2922.

Fairhall, A. L., Lewen, G. D., Bialek, W. and de Ruyter van Steveninck, R. R. (2001). Efficiency and ambiguity in an adaptive neural code. *Nature* **412**, 787-792.

Fischer, B. J. and Konishi, M. (2008). Variability reduction in interaural time difference tuning in the barn owl. *J. Neurophysiol.* **100**, 708-715.

Griss, C. and Rowell, C. H. F. (1986). Three descending interneurons reporting deviation from course in the locust. I. Anatomy. *J. Comp. Physiol. A* **158**, 765-774.

Haag, J. and Borst, A. (1997). Encoding of visual motion information and reliability in spiking and graded potential neurons. *J. Neurosci.* **17**, 4809-4819.

Haag, J. and Borst, A. (1998). Active membrane properties and signal encoding in graded potential neurons. *J. Neurosci.* **18**, 7972-7986.

Haag, J., Wertz, A. and Borst, A. (2007). Integration of lobula plate output signals by DNOVS1, an identified premotor descending neuron. *J. Neurosci.* **27**, 1992-2000.

Hensler, K. (1992). Neuronal co-processing of course deviation and head movements in locusts. I. Descending movement detectors. *J. Comp. Physiol. A* **171**, 257-271.

Hensler, K. and Rowell, C. H. F. (1990). Control of optomotor responses by descending deviation detector neurones in intact flying locusts. *J. Exp. Biol.* **149**, 191-205.

Judge, S. J. and Rind, F. C. (1997). The locust DCMD, a movement-detecting neurone tightly tuned to collision trajectories. *J. Exp. Biol.* **200**, 2209-2216.

Juusola, M. and French, A. S. (1997). The efficiency of sensory information coding by mechanoreceptor neurons. *Neuron* **18**, 959-968.

Kien, J. (1974). Sensory integration in the locust optomotor system, II. Direction selective neurons in the circumoesophageal connectives and the optic lobe. *Vis. Res.* **14**, 1255-1268.

Levi, R. and Camhi, J. M. (2000). Population vector coding by the giant interneurons of the cockroach. *J. Neurosci.* **20**, 3822-3829.
Lewen, G. D., Bialek, W. and de Ruyter van Steveninck, R. R. (2001). Neural coding of naturalistic motion stimuli. *Network* **12**, 317-329.
Liebenthal, E., Uhlman, O. and Camhi, J. M. (1994). Critical parameters of the spike trains in a cell assembly: coding of turn direction by the giant interneurons of the cockroach. *J. Comp. Physiol. A* **174**, 281-296.
Liu, R. C., Tzonev, S., Rebrik, S. and Miller, K. D. (2001). Variability and information in a neural code of the cat lateral geniculate nucleus. *J. Neurophysiol.* **86**, 2789-2806.
Mason, A. C., Oshinsky, M. L. and Hoy, R. R. (2001). Hyperacute directional hearing in a microscale auditory system. *Nature* **410**, 686-690.
Misizin, A. P. and Josephson, R. K. (1987). Mechanical power output of locust flight muscle. *J. Comp. Physiol. A* **160**, 413-419.
Montemurro, M. A., Panzeri, S., Maravall, M., Alenda, A., Bale, M. R., Brambilla, M. and Petersen, R. S. (2007). Role of precise spike timing in coding of dynamic vibrissa stimuli in somatosensory thalamus *J. Neurophysiol.* **98**, 1871-1882.
Nemenman, I., Lewen, G. D., Bialek, W. and de Ruyter van Steveninck, R. R. (2008). Neural coding of natural stimuli: information at sub-millisecond resolution. *PLoS Comput. Biol.* **4**, e1000025.
Nirenberg, S., Carcieri, S. M., Jacobs, A. L. and Latham, P. E. (2001). Retinal ganglion cells act largely as independent encoders. *Nature* **411**, 698-701.
Nolen, T. G. and Hoy, R. R. (1984). Initiation of behaviour by single neurons: the role of behavioural context. *Science* **226**, 992-994.
Petersen, R. S., Panzeri, S. and Diamond, M. E. (2001). Population coding of stimulus location in rat somatosensory cortex. *Neuron* **32**, 503-514.
Peron, S. and Gabbiani, F. (2009). Spike frequency adaptation mediates looming stimulus selectivity in a collision-detecting neuron. *Nat. Neurosci.* **12**, 318-326.
Pollak, G. D., Marsh, D., Bodenhamer, R. and Souther, A. (1977). Characteristics of phasic-on neurons in the inferior colliculus of unanaesthetised bats with observations relating to mechanisms of echo ranging. *J. Neurophysiol.* **40**, 926-942.
Ramirez, J. M. and Pearson, K. G. (1991). Octopaminergic modulation of interneurons in the flight system of the locust. *J. Neurophysiol.* **166**, 1522-1537.
Reinagel, P. and Reid, R. C. (2000). Temporal coding of visual information in the thalamus. *J. Neurosci.* **20**, 5392-5400.
Rieke, F., Warland, D., de Ruyter van Steveninck, R. R. and Bialek, W. (1997). Spikes: exploring the neural code. Cambridge, MA: MIT Press.
Rind, F. C. (1983). A directionally sensitive motion detecting neurone in the brain of a moth. *J. Exp. Biol.* **102**, 253-271.
Rind, F. C. (1990). A directionally selective motion-detecting neurone in the brain of the locust: physiological and morphological characterization. *J. Exp. Biol.* **149**, 1-19.
Rind, F. C. and Simmons, P. J. (1992). Orthopteran DCMD neuron – a reevaluation of responses to moving-objects. I. Selective responses to approaching objects. *J. Neurophysiol.* **68**, 1654-1666.
Rind, F. C., Santer, R. D. and Wright, G. A. (2008). Arousal facilitates collision avoidance mediated by a looming sensitive visual neuron in a flying locust. *J. Neurophysiol.* **100**, 670-680.
Rokem, A., Watzl, S., Gollisch, T., Stemmler, M., Herz, A. V. M. and Samengo, I. (2006). Spike-timing precision underlies the coding efficiency of auditory receptor neurons. *J. Neurophysiol.* **95**, 2541-2552.
Rose, G. and Heiligenberg, W. (1985). Temporal hyperacuity in the electric sense of fish. *Nature* **318**, 178-180.
Rowell, C. H. F. and Pearson, K. G. (1983). Ocellar input to the flight motor system of the locust-structure and function. *J. Exp. Biol.* **103**, 265-288.
Rowell, C. H. F. and Reichert, H. (1986). Three descending interneurons reporting deviation from course in the locust. II. Physiology. *J. Comp. Physiol. A* **158**, 775-794.
Santer, R. D., Rind, F. C., Stafford, R. and Simmons, P. J. (2006). The role of an identified looming-sensitive neuron in triggering a flying locust's escape. *J. Neurophysiol.* **95**, 3391-3400.
Shannon, C. E. and Weaver, W. (1949). *The Mathematical Theory of Information.* Urbana: University of Illinois Press.
Simmons, P. J. (1980). A locust wind and ocellar brain neurone. *J. Exp. Biol.* **85**, 281-294.
Simmons, P. J. (1981). Synaptic transmission between second- and third-order neurones of a locust ocellus. *J. Comp. Physiol.* **145**, 265-276.
Simmons, P. J. (1982). Transmission mediated with and without spikes at connections between large 2nd-order neurons of locust ocelli. *J. Comp. Physiol.* **147**, 401-414.
Simmons, P. J. (1986). Interactions made by large 2nd-order neurons of the median ocellus of the locust. *J. Comp. Physiol. A* **159**, 97-105.
Simmons, P. J. (1990). The effects of temperature on locust ocellar L-neurons and their interconnections. *J. Comp. Physiol. A* **166**, 575-583.
Simmons, P. J. (1993). Adaptation and responses to changes in illumination by 2nd-order and 3rd-order neurons of locust ocelli. *J. Comp. Physiol. A* **173**, 635-648.
Simmons, P. J. (1995). The transfer of signals from photoreceptor cells to large 2nd-order neurons in the ocellar visual-system of the locust *Locusta migratoria*. *J. Exp. Biol.* **198**, 537-549.
Simmons, P. J. (2002). Presynaptic depolarization rate controls transmission at an invertebrate synapse. *Neuron* **35**, 749-758.
Simmons, P. J. and de Ruyter van Steveninck, R. R. (2005). Reliability of signal transfer at a tonically transmitting, graded potential synapse of the locust ocellar pathway. *J. Neurosci.* **25**, 7529-7537.
Strong, S. P., Koberle, R., de Ruyter van Steveninck, R. R. and Bialek, W. (1998). Entropy and information in neural spike trains. *Phys. Rev. Lett.* **80**, 197-200.
Taylor, G. K. and Zbikowski, R. (2005). Nonlinear time-periodic models of the longitudinal flight dynamics of desert locusts *Schistocerca gregaria*. *J. R. Soc. Interface* **2**, 197-221.
van Rullen, R., Guyonneau, R. and Thorpe, S. J. (2005). Spike times make sense. *Trends Neurosci.* **28**, 1-4.
Vogel, A., Hennig, R. M. and Ronacher, B. (2005). Increase of neuronal response variability at higher processing levels as revealed by simultaneous recordings. *J. Neurophysiol.* **93**, 3548-3559.
Warzecha, A. K., Kretzberg, J. and Egelhaaf, M. (1998). Temporal precision of the encoding of motion information by visual interneurons. *Curr. Biol.* **26**, 359-368.
Weis-Fogh, T. (1956). Biology and physics of locust flight. II. Flight performance of the desert locust (*Schistocerca gregaria*). *Philos. Trans. R. Soc. B. Biol. Sci.* **239**, 459-510.
Wertz, A., Borst, A. and Haag, J. (2008). Nonlinear integration of binocular optic flow by DNOVS2, a descending neuron of the fly. *J. Neurosci.* **28**, 3131-3140.
Wilson, M. (1978a). The functional organisation of locust ocelli. *J. Comp. Physiol.* **124**, 297-316.
Wilson, M. (1978b). Generation of graded potential signals in the second order cells of locust ocellus. *J. Comp. Physiol.* **124**, 317-331.
Wilson, M. (1978c). The origin and properties of discrete hyperpolarising potentials in the second order cells of locust ocellus. *J. Comp. Physiol.* **128**, 347-358.